

**Manuscript version: Author's Accepted Manuscript**

The version presented in WRAP is the author's accepted manuscript and may differ from the published version or Version of Record.

**Persistent WRAP URL:**

<http://wrap.warwick.ac.uk/135690>

**How to cite:**

Please refer to published version for the most recent bibliographic citation information. If a published version is known of, the repository item page linked to above, will contain details on accessing it.

**Copyright and reuse:**

The Warwick Research Archive Portal (WRAP) makes this work by researchers of the University of Warwick available open access under the following conditions.

Copyright © and all moral rights to the version of the paper presented here belong to the individual author(s) and/or other copyright owners. To the extent reasonable and practicable the material made available in WRAP has been checked for eligibility before being made available.

Copies of full items can be used for personal research or study, educational, or not-for-profit purposes without prior permission or charge. Provided that the authors, title and full bibliographic details are credited, a hyperlink and/or URL is given for the original metadata page and the content is not changed in any way.

**Publisher's statement:**

Please refer to the repository item page, publisher's statement section, for further information.

For more information, please contact the WRAP Team at: [wrap@warwick.ac.uk](mailto:wrap@warwick.ac.uk).

# Influence of Pole-pair Combinations on the Characteristics of the Brushless Doubly Fed Induction Generator

Ashknaz Oraee, *Member, IEEE*, Richard McMahon, Ehsan Abdi, *Senior Member, IEEE*,  
Salman Abdi, *Member, IEEE*, and Sul Ademi, *Member, IEEE*,

**Abstract**—The brushless doubly fed induction generator (BDFIG) is an alternative to the doubly fed induction generator (DFIG), widely used in wind turbines which avoids the need for brush gear and slip rings. The choice of pole numbers for the two stator windings present in the BDFIG sets the operating speed, typically in the medium speed range to eliminate a gearbox stage. This paper focuses on how both the total number of poles and the assignment of poles between the windings affect machine performance. Analytical expressions have been developed for parameters including pull-out torque, magnetizing current and back-iron depth. The results show that the pole count can be increased without unduly compromising pull-out torque and that in cases where more than one combination of pole number is acceptable only the back iron depth is significantly affected. In addition an output factor has been introduced to enable a direct comparison to be made with conventional DFIGs. The torque density of a brushless DFIG is compromised to a degree relative to a comparable DFIG as a consequence of the presence of two magnetic fields and finite element analysis is needed to achieve an optimized design. Finally, predictions of the performance of multi-MW machines are made based on data from an existing 250 kW machine which show that suitable efficiencies can be obtained and excessive control winding excitation can be avoided.

**Index Terms**—Brushless doubly-fed generator (BDFG), electrical machine design, induction generator, power factor, pole-pair.

## NOMENCLATURE

$p_1, p_2$	stator winding pole-pairs (principal fields)
$g$	air gap length
$n_r, n_{r_{opt}}$	rotor turns ratio, general and optimal
$f, f_1, f_2$	frequency stator windings 1, 2
$l, d$	stack length, air gap diameter
$\omega_r$	rotor angular velocity
$B_1, B_2$	rms value of flux density stator windings 1, 2

$N_1, N_2$	number of turns stator windings 1, 2
$B_c$	peak flux density in core
$y_c$	back iron depth
$\omega_r$	rotor angular velocity
$\bar{B}$	magnetic loading
$\bar{J}$	electric loading

## I. INTRODUCTION

THE brushless DFIG is an alternative to the well-established doubly fed induction generator (DFIG) for use in wind turbines, since it offers improved reliability and reduced capital and maintenance costs [1]. It retains the low-cost advantage of the DFIG system as it only requires a fractionally rated converter and does not use permanent magnet materials. The machine has no brushed contact to the rotor, eliminating a common source of failures, making it a particularly attractive machine for offshore wind turbines. Moreover, the brushless DFIG is intrinsically a medium-speed machine, enabling the use of a simplified one or two-stage gearbox as shown in Fig. 1.

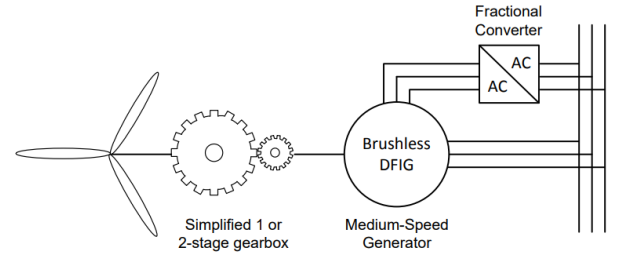


Fig. 1. Brushless DFIG drivetrain set-up for wind power applications.

The brushless DFIG has its origins in the self-cascaded machine and has two non-coupling stator windings, referred to as the power winding (PW) and the control winding (CW) with different pole numbers,  $p_1$  and  $p_2$  creating two stator fields in the machines magnetic circuit with different frequencies and pole numbers [2]. A specially designed rotor couples to both stator windings. Applications other than wind power have been considered for this machine, for instance as a stand-alone generator for off-grid applications [3], a drive in pump applications [4] and in shaft generator systems for ships [5].

An alternative approach is the brushless doubly-fed reluctance generator (BDFRG) in which the short-circuited coils in the rotor of the brushless DFIG are replaced by high-reluctance

Manuscript received February 26, 2019; revised September 16, 2019, January 25, 2020; accepted February 12, 2020. This work was supported by the European Union's Seventh Framework Program managed by Research Executive Agency under Grant Agreement N.315485. Paper no. TEC-00211-2019. (Corresponding author: Sul Ademi)

A. Oraee is with the Department of Engineering, University of Cambridge, Cambridge, CB2 1PZ, U.K. (e-mail: ashknaz.oraee@gmail.com)

E. Abdi is with the Wind Technologies Limited, St. John's Innovation Centre, Cambridge, U.K. (e-mail: ehsan.abdi@windtechnologies.com)

S. Abdi is with the School of Engineering, University of East Anglia, Norwich, NR4 7TJ, U.K. (e-mail: S.abdi-jalebi@uea.co.uk)

S. Ademi and R. McMahon are with the Warwick Manufacturing Group (WMG), The University of Warwick, Coventry, CV4 7AL, U.K. (e-mail: S.Ademi@warwick.ac.uk and R.McMahon.1@warwick.ac.uk)

Color versions of one or more of the figures in this paper are available online at <http://ieeexplore.ieee.org>

flux barriers [6]. It has been shown that any rotor type used for synchronous reluctance machines (SynRMs) is essentially applicable in the BDFRG, i.e., the simple salient-pole rotor [7], axially-laminated anisotropic rotor [8] and multi-layer flux-barrier rotor [9]. The BDFRG alternative has been widely taken into consideration [10] and several design modifications [11] and control optimizations have been proposed [12], [13]. This paper will, however, limit its scope to the brushless DFIG.

The design of the brushless DFIG is not straightforward since there are more variables to consider than in conventional induction machine designs [14]. Attention has been given to some aspects of design for wind power applications as reported in [15]–[18] and several large machines have been reported. These include a 75 kW machine [17], a 200 kW machine [19] and the 250 kW machine built and tested by the authors of [20]. This latter, believed to be the largest to date, was conceived as a stepping-stone towards commercial MW scale brushless DFIGs. In a wind turbine application, the machine will be matched to the rest of the drivetrain so the natural speed, dependent on the sum of the pole-pairs, and the speed range around natural speed, typically  $\pm 30\%$ , are of interest.

This paper examines how the characteristics and performance of the machine are affected by the choice of pole-pairs, and the allocation of these to the two windings. Although some design relationships were developed in [21], important characteristics such as pull-out torque, back-iron depth and magnetizing current were not considered. In particular, this paper considers the trends in these parameters as a function of natural speed, as set the pole numbers.

It was shown in [22] that to achieve the required performance for wind turbine service, namely a power factor in the range of 0.95 lag to 0.95 lead, the CW of the 250 kW machine considered needed to be significantly over-excited, compromising machine output. The rotor leakage inductance is particularly significant in setting the required degree of over-excitation. The final section of this paper looks at the performance trends of future medium-speed MW scale brushless DFIGs. The presence of two stator windings means that there are more variables to consider than in a single winding machine especially when it comes to control and stability. The dynamics, control and stability of the machine have been reported in [20] and low voltage ride through (LVRT) performance was considered in [23].

This paper is organized as follows. Section II describes the brushless DFIG operation and the per-phase equivalent circuit. The pole-number choice and effect on machine rating are presented in section III. The effect of pole-pair split on machine fields and back-iron considerations are reported in section IV. Section V details the amp-turns ratios for common  $(p_1/p_2)$  pole-pair. Performance analysis of the 4/8 frame size of the D400 prototype, the pull-out torque, power factor and efficiency are detailed in section VI. Optimization design for the megawatt (MW) BDFRGs are explored and brought into focus in Section VII. Finally, Section VIII draws conclusions.

## II. BRUSHLESS DFIG OPERATION

The brushless DFIG normally operates in the synchronous mode in which the shaft speed is independent of the torque

exerted on the machine, as long as it is smaller than the pull-out torque. The speed is determined by the frequency and pole-pair numbers of the stator windings and is given by:

$$N_r = \frac{60(f_1 + f_2)}{p_1 \pm p_2} \quad (1)$$

where  $f_1$  and  $f_2$  are the frequencies of the supplies to the stator windings,  $p_1$  and  $p_2$  are the pole-pair numbers of the windings.

### A. Brushless DFIG equivalent circuit

The operation of the BDFG can be described by a per-phase equivalent circuit [22] similar to the equivalent circuits of two induction machines with interconnected rotors, as shown in Fig. 2. In the figure  $R_1$  and  $R_2$  are the stator resistances,  $L_{m1}$  and  $L_{m2}$  are the stator magnetizing inductances and  $L_1$  and  $L_2$  are the stator leakage inductances. Parameters are referred to the PW using the modifier “’”. Furthermore, the rotor can be characterized by the rotor turns ratio  $n_r$ , resistance  $R_r$  and leakage inductance  $L_r$ , the two latter parameters are also shown in the referred per-phase equivalent circuit of Fig. 2.

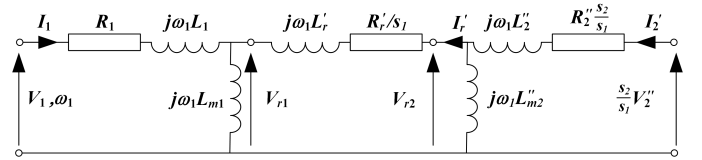


Fig. 2. Referred per-phase equivalent circuit of the brushless DFIG.

The rotor leakage inductance includes conventional leakage elements but the space harmonics associated with common designs of brushless DFIG rotors lead to a higher differential leakage component compared to conventional induction machine rotors. The slips  $s_1$  and  $s_2$  are defined as in [1].

## III. POLE-NUMBER CHOICE

### A. Choice of pole numbers

For  $(p_1 + p_2)$  type brushless DFIGs, the choice of stator winding pole-pair numbers to give a desired natural speed, hence operating speed range, is the first step in the design process. The sum of the pole-pair combination, rounded to the nearest integer, is given by:

$$p_1 + p_2 = \frac{60f_1}{N_r} \quad (2)$$

Both the total pole-pair count and the split between the windings affect machine performance. Direct coupling between the two stator windings must be avoided and this can be achieved by applying the rules given in [21]. This paper considered a range of design considerations, including the choice of pole-pair numbers, and provided experimental validation from a D180 machine. Moreover, [21] identified a number of factors to be taken into account in the design of a BDFG and these were validated by experimental data for the D180 brushless DFIG. In some cases, several pole number combinations are possible and there is the choice of giving the

higher or lower pole number to the PW. The torque capability of a brushless DFIG collapses as the speed of the machine approaches the synchronous speed of the PW. Thus, for the widest speed range, the lower pole number should be assigned to the PW and the frequency of the rotor currents is reduced in this connection. However, if the operating speed range is limited to  $\pm 30\%$  around natural speed, as in wind power applications, this constraint does not apply. Furthermore, some pole-pair combinations lead to unwanted unbalanced magnet pull and vibration effects. When there is more than one permissible combination of pole-pair numbers, the machine design can be modified to give a trade-off between output torque, speed, and magnetization considerations as evaluated in the following sections.

#### B. Effect on machine rating

An expression for the power rating of the BDFG, calculated from the equivalent circuit model, was derived in [1]. This expression was based on the quadrature sum ( $B_{quad}$ ) of the two fields in the machine but an alternative approach taking a more conservative view of the maximum allowable fields was developed in [21] based on the simple sum of the fields. Both relationships are given in the Appendix. Unfortunately, there is at present no easy way of determining the maximum tolerable fields in the machine, but experience suggests that  $B_{sum}$  is too conservative [24]. The two assumptions do, however, appear in practice to bracket the range of allowable flux densities, hence both are considered. Certain other assumptions are used in the expressions for power rating, the most relevant here is that only synchronous torques are produced and that the voltage drop across the rotor is not significant.

As the output power is proportional to the speed, it is instructive to normalize the output of the brushless DFIG to that of a DFIG with a synchronous speed equal to the natural speed of the brushless DFIG, both machines having the same rotor dimensions. The induction machine therefore has  $(p_1 + p_2)$  poles [25]. This leads to expressions for an output factor, in effect the ratio of available torque to that of the equivalent DFIG, again as derived in the Appendix. The output factor is a measure of performance that can be used to compare different machine designs. The expression depends on the rotor turns ratio  $n_r$ , but can be evaluated using a value equal to the optimum value as given in the Appendix. In the case of the simple sum basis it reduces to:

$$Output\ factor = \frac{T_{BDFG}}{T_{IM}} = \frac{1 + \frac{p_2}{p_1}}{(1 + (\frac{p_2}{p_1})^{\frac{1}{2}})^2} \quad (3)$$

The corresponding expression based on the quadrature sum method is:

$$Output\ factor = \frac{T_{BDFG}}{T_{IM}} = \frac{1 + \frac{p_2}{p_1}}{(1 + (\frac{p_2}{p_1})^{\frac{2}{3}})^{\frac{3}{2}}} \quad (4)$$

The output factors for common  $(p_1/p_2)$  brushless DFIGs are given in Table I, showing that the higher the ratio of pole numbers, the greater the output factors can be obtained. This implies that the relative output is at minimum when  $p_1 = p_2$ , recognizing that such a machine is impractical, as noted in

[26]. Using the sum of fields assumption, the minimum output torque is 50% of that of a  $(p_1 + p_2)$  induction machine but this rises to nearly 54% for the 2/6 pole configuration. For comparison, the quadrature sum method gives substantially higher output factors, as shown in Table I.

TABLE I  
OUTPUT FACTOR FOR VARIOUS POLE NUMBER OF BRUSHLESS DFIG

$(p_1/p_2)$	$n_{r_{opt}}$ ( <i>sum</i> )	$n_{r_{opt}}$ ( <i>quad</i> )	Output factor ( <i>sum</i> )	Output factor ( <i>quad</i> )
2/6	0.577	0.48	0.536	0.74
8/12	0.816	0.76	0.505	0.71
4/8	0.707	0.53	0.515	0.72
2/8	0.5	0.40	0.556	0.76
2/10	0.45	0.34	0.573	0.77

### IV. MAGNETIC CIRCUIT CONSIDERATIONS

#### A. Effect of pole-pair split on machine fields

It was shown in [1] that the two fields in a brushless DFIG mode are related by the rotor turns ratio, pole numbers and voltage drop across the rotor leakage inductance. If it is assumed that this drop is small, then the ratio of the two fields is given by:

$$\frac{B_2}{B_1} = n_r \frac{p_2}{p_1} \quad (5)$$

where  $B_1$  and  $B_2$  are the RMS values of the fundamental  $p_1$  and  $p_2$  pole-pair air gap flux densities. However, in reality there can be a significant voltage across the rotor impedance, especially when the machine is over-excited, hence (5) is no longer valid. Over-excitation is particularly likely in smaller machines to achieve an acceptable grid-side power factor [22]. In this study, the CW voltage is limited to avoid undue over-excitation.

#### B. Back-iron considerations

The back-iron flux in conventional induction machines is defined as half of the total flux over one pole pitch. The peak flux density in stator or rotor core is then related to the magnetic loading by conservation of flux and for brushless DFIG it can be calculated from:

$$\hat{B}_c = \frac{\sqrt{2}}{2} \frac{d}{y_c} B_{sum} \quad (6)$$

where  $y_c$  is the back-iron depth. The back-iron flux density in the brushless DFIG varies with time and position but a value for the peak can be found using  $B_{sum}$ , which is divided into  $B_1$  and  $B_2$  for  $p_1$  and  $p_2$  fields, respectively, using (5). The back-iron depth for the brushless DFIG is then given by [15]:

$$y_c = \frac{\sqrt{2}}{2} \frac{d}{\hat{B}_c} \left[ \frac{B_1}{p_1} + \frac{B_2}{p_2} \right] \quad (7)$$

For the brushless DFIG the back-iron depth in terms of the total air gap flux density,  $B_{sum}$ , can be found by re-arranging and substituting equations (5) and (6) in (7):

$$y_c = \frac{\sqrt{2}}{2} \frac{d B_{sum}}{\hat{B}_c} \left[ \frac{p_1(1 + \frac{1}{n_r}) + p_2(1 + n_r)}{2p_1p_2 + p_2^2 n_r + p_1^2 \frac{1}{n_r}} \right] \quad (8)$$

Substituting  $n_{r_{opt}}$  from equation (23) then gives:

$$y_c = \frac{\sqrt{2}}{2} d \frac{B_{sum}}{\hat{B}_c} \left[ \frac{(1 + \frac{p_2}{p_1})(1 + 2(\frac{p_2}{p_1})^{\frac{1}{2}} + \frac{p_2}{p_1})}{2(\frac{p_2}{p_1}) + (\frac{p_2}{p_1})^{\frac{1}{2}} + (\frac{p_2}{p_1})^{\frac{3}{2}}} \right] \quad (9)$$

The back-iron depth ratio of the  $(p_1/p_2)$  brushless DFIG to a conventional IM of  $(p_1 + p_2)$  poles is given by:

$$\frac{y_{c_{BDFG}}}{y_{c_{IM}}} = p_1 + (p_2) \left[ \frac{p_1(1 + \frac{1}{n_r}) + p_2(1 + n_r)}{2p_1p_2 + p_2^2n_r + p_1^2(\frac{1}{n_r})} \right] \quad (10)$$

A similar approach gives the ratio of back-iron depths on the basis of the quadrature sum method, given by:

$$\frac{y_{c_{BDFG}}}{y_{c_{IM}}} = (p_1 + p_2) \left[ \frac{p_1(1 + \frac{1}{n_r}) + p_2(1 + n_r)}{2p_1p_2 + p_2^2n_r + p_1^2(\frac{1}{n_r})} \right] \quad (11)$$

The back-iron depth ratios for common  $(p_1/p_2)$  pole-pair brushless DFIGs have been calculated and are given in Table II for both the simple and quadrature sum methods. The peak flux density in the back-iron is limited to 1.8 T.

TABLE II  
BACK-IRON RATIO FOR VARIOUS POLE NUMBERS OF BRUSHLESS DFIG

Brushless DFIG ( $p_1/p_2$ )	$n_{r_{opt}}$ ( <i>sum</i> )	$n_{r_{opt}}$ ( <i>quad</i> )	Back-iron ratio ( <i>sum</i> )	Back-iron ratio ( <i>quad</i> )
2/6	0.577	0.48	2.31	3.37
8/12	0.816	0.76	2.04	3.00
4/8	0.707	0.53	2.12	2.95
2/8	0.5	0.40	2.50	2.69
2/10	0.45	0.34	2.68	2.98

The back-iron ratio is a minimum at  $p_1 = p_2$ , which is not feasible, as noted earlier. The minimum depth is twice of that of a  $(p_1 + p_2)$  induction machine on the simple sum basis, and  $2\sqrt{2}$  times on the quadrature sum basis which, however, gives a higher machine output. As the ratio of pole-pair numbers increases, there is a slight rise in the depth of back-iron required.

The results for a wide range of pole number combinations on the basis of optimum turns ratio calculation for the sum and quadrature sum method are shown in Fig. 3. The BDFG needs more back iron than a corresponding DFIG as the two machine fields have lower pole numbers. However, in any case a certain minimum back iron depth may be mandated by structural considerations. To determine an accurate depth requires finite element analysis to take saturation into account [24].

## V. MAGNETIZATION

### A. Magnetizing amp-turns

For the brushless DFIG the total magnetizing amp-turns ( $AT_{tot}$ ) for the  $p_1$  and  $p_2$  pole-pair fields, assuming that they are in ratio given by equation (5), are given by:

$$AT_{tot} = \frac{2g}{\mu_o} \pi p_1 \left[ \frac{1 + (\frac{p_2}{p_1})^2 n_r}{1 + \frac{p_2}{p_1} n_r} \right] \quad (12)$$

where  $AT_{tot}$  is the product of  $I_{mag} N_{eff}$ ,  $g$  is the air gap length and  $\mu_o$  is the permeability of air. The amp-turns ratio of the

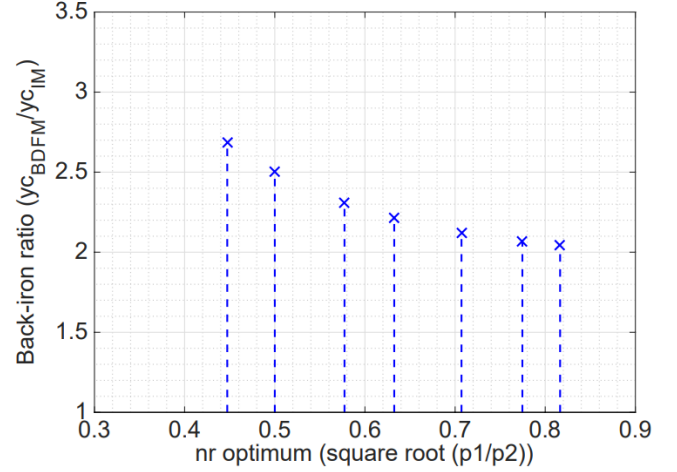


Fig. 3. Back-iron ratio variation with optimum turns ratio.

$(p_1/p_2)$  brushless DFIG to a conventional induction machine of  $p_1 + p_2$  pole-pairs is then:

$$\frac{AT_{BDFG}}{AT_{DFIG}} = \left( \frac{p_1}{p_1 + p_2} \right) \left[ \frac{1 + (\frac{p_2}{p_1})^2 n_r}{1 + \frac{p_2}{p_1} n_r} \right] \quad (13)$$

Substituting  $n_{r_{opt}}$  from equation (23) for the  $B_{sum}$  formulation gives:

$$\frac{AT_{BDFG}}{AT_{DFIG}} = \left( \frac{p_1}{p_1 + p_2} \right) \left[ \frac{1 + (\frac{p_2}{p_1})^{\frac{3}{2}}}{1 + (\frac{p_2}{p_1})^{\frac{1}{2}}} \right] \quad (14)$$

The corresponding expression for the quadrature sum approach and substituting  $n_{r_{opt}}$  from equation (24) is given by:

$$\frac{AT_{BDFG}}{AT_{DFIG}} = \left( \frac{p_1}{p_1 + p_2} \right) \left[ \frac{1 + (\frac{p_2}{p_1})^{\frac{4}{3}}}{1 + (\frac{p_2}{p_1})^{\frac{2}{3}}} \right] \quad (15)$$

The amp-turns ratios for common  $(p_1/p_2)$  pole-pair brushless DFIGs are calculated and given in Table III. From a magnetizing current point of view, this ratio is a minimum at  $p_1 = p_2$ , however but this is impractical. On the simple sum basis the magnetizing amp-turns are 50% of that of a  $(p_1 + p_2)$  induction machine, but the brushless DFIGs torque, according to (18) is only half that of the induction machine, showing that the BDFG requires the same magnetizing  $AT$  per unit torque. Similarly, on a quadrature sum basis, the magnetizing  $AT$  are 70.7% of those of a DFIG, but again the output torque is only 70.7%. Whilst there is an increase in the magnetizing  $AT$  with a greater ratio of pole numbers, there is a corresponding rise in output factor so a  $(p_1/p_2)$  BDFG requires essentially the same magnetizing  $AT$  as a  $(p_1 + p_2)$  DFIG.

TABLE III  
AMP-TURNS RATIO FOR VARIOUS POLE-PAIR BRUSHLESS DFIG

Brushless DFIG pole ratio	$n_{r_{opt}}$	$AT$ ratio ( <i>sum</i> )	$AT$ ratio ( <i>quad</i> )
1/3	0.577	0.567	0.76
2/3	0.816	0.510	0.72
1/2	0.707	0.528	0.73



The amp-turns ratio of the brushless DFIG to the conventional induction machine for various pole-pair ratios using the simple sum method is presented in Fig. 4.

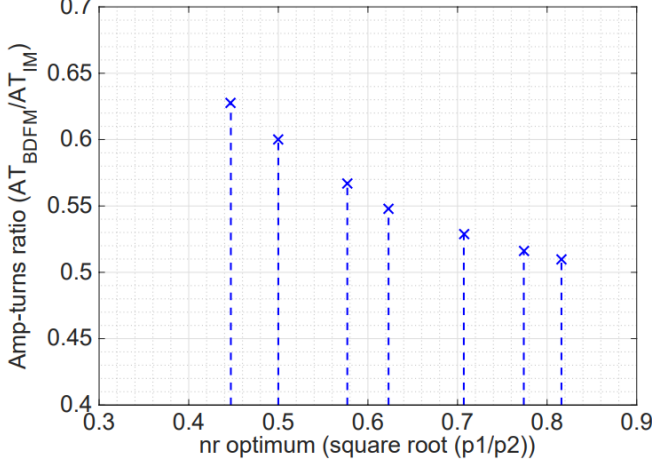


Fig. 4. Amp-turns ratio variation with optimum turns ratio (simple sum).

## VI. PERFORMANCE ANALYSIS AND RESULTS

The foregoing points are examined in the context of an existing frame size D400, 250 kW brushless DFIG [20] by considering designs for different speed options, i.e., pole number combinations. The equivalent circuit model is used to represent the steady-state performance of the machine, offering a straightforward method of calculating the efficiency and power factor to a practical accuracy. The physical dimensions and specifications of the D400 machine together with stator and rotor winding details are given in Table IV.

TABLE IV  
SPECIFICATIONS OF THE 4/8 FRAME SIZE D400 BRUSHLESS DFIG

Physical dimintions			
Stack length, mm	820	Rated power, kW	250
Stator diameter, mm	440	Rated torque, Nm	3670
Stator slots	72	Speed range, rpm	500 $\pm$ 36%
Rotor slots	60	Efficiency	93%
Winding details			
PW poles	4	PW rated voltage	690 (50 Hz)
PW turns	48	PW rated current	94 A
CW poles	8	CW rated voltage	620 (18 Hz)
CW turns	168	CW rated current	40 A

The nested-loop rotor of this machine comprises  $(p_1 + p_2)/2$  sets of nests, each with five loops and the conductors being solid bars with one common end ring. The number of rotor slots, and hence the number of loops, will therefore depend on the pole number count and so the machine will not necessarily be suited for actual production and/or manufacturing.

### A. D400 machines

Designs for common brushless DFIG pole-pair combinations using the same dimensions of the existing D400 prototype machine have been investigated. Table V, provides details of the designs with constant rated torque but different speeds

and hence powers. The PW power factor is set to 0.95 lagging, determining the CW voltage and the balance between  $B_1$  and  $B_2$  is changed by varying number of turns. The total flux density,  $B_{sum}$ , is 0.7 T and peak flux densities in the rotor tooth and back-iron is limited to 1.5 T. All equivalent circuit parameters, including leakage inductances, are recalculated for each new design using the software described in [21].

TABLE V  
DESIGN OF VARIOUS POLE NUMBER BRUSHLESS DFIGS FOR FIXED PW POWER FACTOR OF 0.95 LAGGING

Brushless DFIG design parameters				
Pole ( $p_1/p_2$ )	8/12	4/12	4/8	2/6
$\omega_n$ (rpm)	300	375	500	750
Rated power (kW)	150	187	250	375
Rotor slots	100	80	60	56
Stator slots	72	72	72	72
$N_1$	120	76	66	40
$N_2$	220	210	146	100
$B_1$ (T)	0.230	0.271	0.219	0.218
$B_2$ (T)	0.470	0.429	0.481	0.482
Efficiency	82%	84%	88%	95%
Torque (kNm)	3.7	3.7	3.7	3.7
PW power factor	0.95 lag	0.95 lag	0.95 lag	0.95 lag
Total amp turns	5313	4954	3261	2300

The total stator electric loading is kept at 5.7 kA/m. Furthermore, the number and diameter of the stator conductors and cross-section of the rotor bars are modified such that the total conductor cross-sectional areas are identical to those of the D400 machine. The stator current density is 3.5 A/mm<sup>2</sup> and the rotor current density is 5 A/mm<sup>2</sup>. The air gap diameter and stack length has been kept constant for all pole number designs. It can be seen that the 2/6 pole brushless DFIG has both the highest natural speed, power and efficiency, whilst producing the same torque as the original 4/8 machine. Moreover, this pole-pair configuration requires the lowest total amp-turns for magnetization, but needs the highest back iron depth as shown in Table VI.

TABLE VI  
BACK IRON DESIGN OF VARIOUS POLE NUMBER BRUSHLESS DFIGS

Brushless DFIG pole ( $p_1/p_2$ )	$n_r$	$B_1$ (T)	$B_2$ (T)	$y_c$ (mm)
2/6	0.53	0.27	0.43	71
4/8	0.68	0.29	0.41	43
4/12	0.53	0.27	0.43	36
8/12	0.80	0.32	0.38	25

To reduce the depth of back iron, the  $B_{sum}$  limit can be increased from 0.7 T to 0.8 T, without undue increase in magnetizing current, as seen in Table VII, which shows designs of the D400 brushless DFIG for higher  $B_{sum}$  for a constant torque of 3670 Nm. As stated in (5), the distribution of  $B_1$  and  $B_2$  fields are dependent on the rotor turns ratio and the stator windings number of pole-pairs. Due to the change in the number of PW and CW turns, the total amp-turns is also changed. In the redesigns, conductor current densities, slot dimensions and slot fill are kept constant. The peak flux

densities in the rotor tooth and back-iron are limited to 1.6 T and 1.7 T, respectively.

TABLE VII  
DESIGN OPTIMIZATION OF THE 4/8 D400 BDFIG FOR INCREASED  $B_{sum}$

4/8 D400 BDFIG	$B_{sum} = 0.7$ T	$B_{sum} = 0.75$ T	$B_{sum} = 0.8$ T
$B_1$ (T)	0.219	0.230	0.250
$B_2$ (T)	0.481	0.520	0.550
$N_1$	66	62	57
$N_2$	146	134	127
Efficiency	88%	89%	90%
PW power factor	0.95 lag	1	1
Total amp turns	3261	3517	3704

As evident from Table VII, unity PW power factor can be achieved at rated design CW voltage of 620 V for the 250 kW brushless DFIG by increasing the total flux density in the air gap. To obtain unity PW power factor for a  $B_{sum}$  of 0.75 T and 0.8 T,  $B_1$  is increased by 20% and 14%, respectively.

### B. Pull-out torque of D400 machines

From the previous section, the theoretically available maximum running torque depends to a degree on total pole count, as well as the split of pole numbers. However, a further consideration is the load angle at which the machine operates, related in turn to the pull-out torque. For well-known reasons, operation away from pull-out is desirable. In the BDFG, the pull-out torque is primarily determined by the rotor inductance and this was believed to increase with pole count [15].

To investigate the effect, brushless DFIGs were designed with the same overall rotor dimensions, starting from the well-characterized 250 kW D400 frame size machine [20], for different pole numbers using the design methodology reported in [21]. The stator windings were configured to use the same number of stator slots and the rotor slots are chosen to give enough conductor area for the stator electrical loading to be balanced, with the same current density in the rotor conductors as the previous section. The design program calculates machine parameters, notably the rotor leakage inductance, taking into account space harmonic effects and the couplings between the rotor loops using simple sum analysis method.

Figure 5, shows the variation of pull-out torque for BDFGs with different natural speeds and in ascending order corresponding to 8/12, 4/12, 4/8 and 2/6 pole machines. As shown the 4/8 and 2/6 pole machines with natural speeds of 500 and 750 rpm, respectively, offer somewhat higher pull-out torques allowing easier control and improved stability due to lower rotor leakage inductance,  $L_r$ . When designing high pole count machines, there is a need to pay careful attention to keeping the rotor inductance down to an acceptable level to retain a suitable margin of pull-out torque relative to the normal running torque but this is seen to be achievable at least to a total pole count of twenty. The normal running full load torque for designs with natural speeds of 300, 375, 500 and 750 rpm is 3.7 kNm.

### C. Power factor

Achieving a good power factor is important and increasingly wind turbines are expected to contribute to the VARs. The

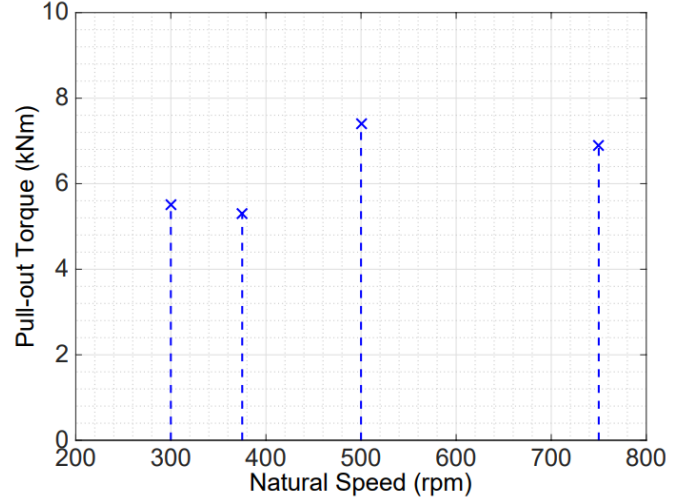


Fig. 5. Pull-out torque variation with natural speed and normal running torque of 3.7 kNm.

selection of machine speed, and hence pole-pair count has a significant effect on machine operating conditions. Fig. 6, shows the variation of the PW power factor for sums of  $p_1$  and  $p_2$  pole-pairs at balanced excitation (minimum rotor currents), preferred for low losses. It has been found that brushless DFIGs with a lower sum pole-pairs and higher PW power factors can be achieved. The designs used in Fig. 6 are those in Table V, which were designed to be capable of operating at a fixed power factor of 0.95 lagging; parameters are given in the Appendix.

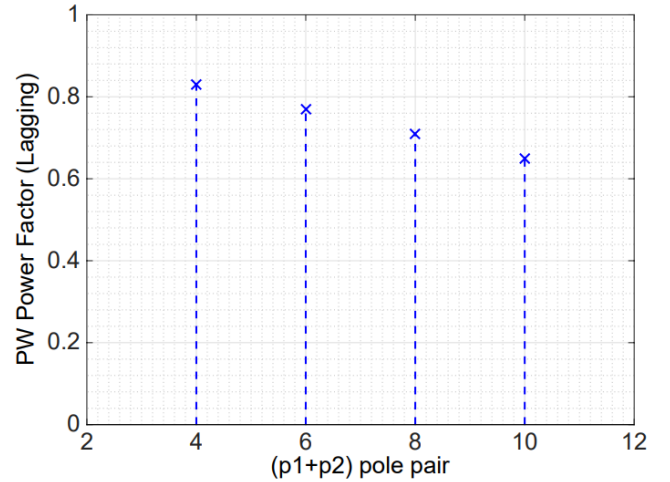


Fig. 6. PW power factor variation with sum of pole-pairs at rated torque and speed.

### D. Efficiency

Figure 7, shows the variation of efficiency as the PW power factor is improved for the existing 250 kW BDFG prototype. Achieving a higher PW power factor comes at a price of reduced efficiency, illustrating the trade-off between satisfying power factor requirements and other performance measures.

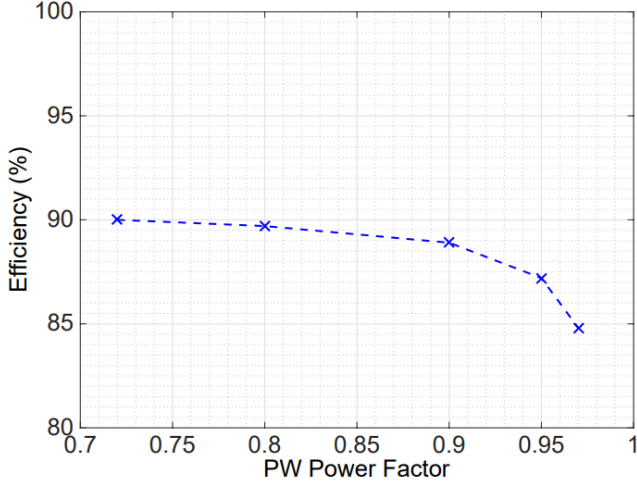


Fig. 7. Efficiency variation with PW power factor for 250 kW BDFIG.

## VII. MEGAWATT MACHINES

The intention is, of course, to deploy the brushless DFIG in large wind turbines, so it is important to know how such a machine would operate. According to recent grid codes, wind farms have to supply reactive as well as real power to the grid. For a brushless DFIG the power factor can be controlled by the converter feeding the control winding, but as noted in [22] there are some practical limits. To explore the expected performance of large machines, designs have been developed for 2.5 MW and 5 MW medium speed machines as tabulated in Table VIII. The proportionately lower rotor leakage reactance allows unity PW power factor to be achieved in both machines at rated CW design voltages without increasing  $B_{sum}$ , therefore has been kept at 0.7 T.

TABLE VIII  
OPTIMIZED DESIGNS FOR MW BRUSHLESS DFIGS

Brushless DFIG design parameters		
	2.5 MW	5 MW
Pole ( $p_1/p_2$ )	4/8	8/12
Stack length (mm)	920	800
Air gap diameter (mm)	1065	1965
$\omega_n$ (rpm)	500	300
Speed range (rpm)	320-680	192-408
Rated power (MW)	2.5	5
Rated PW voltage (V)	690 at 50 Hz	690 at 50 Hz
Rated CW voltage (V)	660	620
Rotor slots	60	140
Stator slots	72	72
$B_1$ (T)	0.275	0.290
$B_2$ (T)	0.425	0.410
$N_1$	18	20
$N_2$	72	52
Efficiency	96%	97%
Torque (kNm)	38.4	120
PW power factor	1	1
Total amp turns	6542	8020

Figure 8, illustrates the PW power factor variation with respect to the rated output power as machine size increases.

The machines are taken from Table V and Table VIII, noting that they have different pole numbers. Each data point was recorded for a balanced excitation condition, with each winding providing its own magnetizing current. This condition was achieved by adjusting the CW voltage to minimize the rotor currents, for a given PW voltage, at full load operating conditions.

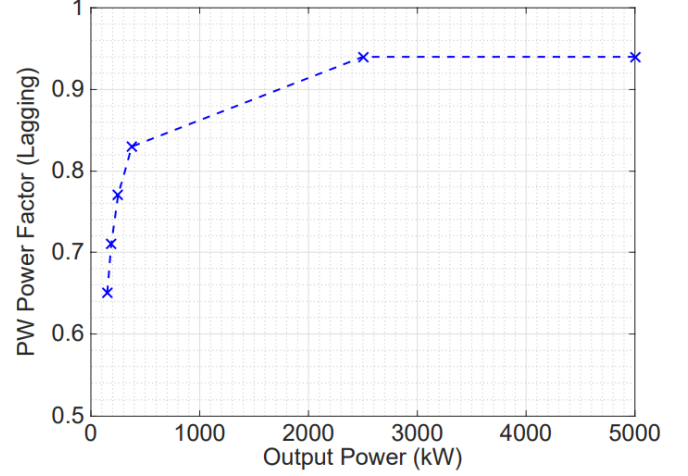


Fig. 8. PW power factor variation with respect to the rated output power.

It is evident that smaller machines suffer from lower power factors without an excessively high CW voltage. A line side converter with a higher rating or capacitor banks at grid terminals can be used to contribute to the generation of reactive power. However, the problem becomes less critical for larger machines, since the per unit value of the rotor reactance drops with size [27]. For the designs considered, a worst case PW power factor of 0.95 lagging is achieved at balanced excitation and a modest degree of over-excitation of the CW will enable the export of VARs to the grid.

## VIII. CONCLUSIONS

This paper has examined the effect of the number of poles and pole-pair combinations on the performance of the brushless DFIG, especially in the context of future MW scale machines. The analysis presented in the paper shows that acceptable pull-out torques can be maintained for machines with natural speeds in the range examined, namely 300 to 750 rpm, i.e., with pole counts from 8 to 20. The split of pole numbers between the two windings in cases where more than one combination is acceptable does not significantly affect the pull-out torque. For the same output power and speed, the brushless DFIGs require essentially the same magnetizing ampere-turns as conventional DFIGs and the magnetizing current does not change significantly with the split of pole numbers. As with conventional machines, the back-iron depth reflects the choice of pole numbers, and if a 2-pole winding is present a significantly higher back iron depth is needed.

This paper has used both simple and quadrature sum approaches for the two fields, but the trends noted above are not dependent on the approach adopted. However, the machine's



output does reflect the maximum allowable flux density and finite element analysis is need to achieve an optimized design. Encouragingly, designs for brushless DFIGs up to 5 MW, based on the performance of the existing 250 kW machine show that a good power factor can be achieved without excessive excitation of the control winding or compromising efficiency.

#### APPENDIX A

The power rating of the brushless DFIG, calculated from the equivalent circuit model, was derived in [1] based on the quadrature sum of fields and is given by:

$$P_{quad} = \frac{\pi^2}{\sqrt{2}} \left( \frac{d}{2} \right)^2 l \omega_r \overline{B} J \left[ \frac{p_1 + p_2}{p_1 \left( 1 + \frac{1}{n_r} \right) \left( 1 + \left( n_r \frac{p_2}{p_1} \right)^2 \right)^{\frac{1}{2}}} \right] \quad (16)$$

The power rating of a conventional induction machine with  $(p_1 + p_2)$  pole-pairs is found from:

$$P_{IM} = \frac{\pi^2}{\sqrt{2}} \left( \frac{d}{2} \right)^2 l \overline{B} J \left[ \frac{\omega_s}{p_1 + p_2} \right] \quad (17)$$

The output power is then calculated as:

$$\frac{P_{quad}}{P_{IM}} = \left[ \frac{p_1 + p_2}{p_1 \left( 1 + \frac{1}{n_r} \right) \left( 1 + \left( n_r \frac{p_2}{p_1} \right)^2 \right)^{\frac{1}{2}}} \right] \quad (18)$$

Using the alternative  $B_{sum}$  approach, for the brushless DFIG, maximum output power can be calculated as:

$$P_{B_{sum}} = \frac{\pi^2}{\sqrt{2}} \left( \frac{d}{2} \right)^2 l \omega_r \overline{B} J \left[ \frac{1}{p_1 \left( 1 + \frac{1}{n_r} \right) + \left( 1 + n_r \frac{p_2}{p_1} \right)} \right] \quad (19)$$

Hence, output power ratio is then calculated as:

$$\frac{P_{B_{sum}}}{P_{IM}} = \left[ \frac{p_1 + p_2}{p_1 \left( 1 + \frac{1}{n_r} \right) + \left( 1 + n_r \frac{p_2}{p_1} \right)} \right] \quad (20)$$

These powers can be normalised to the output of a  $p_1 + p_2$  DFIG leading to output factor of:

$$Output\ factor = \frac{T_{BDFIG}}{T_{IM}} \left[ \frac{1 + \frac{p_2}{p_1}}{\left( 1 + \frac{1}{n_r} \right) \left( 1 + \left( n_r \frac{p_2}{p_1} \right)^2 \right)^{\frac{1}{2}}} \right] \quad (21)$$

For the quadrature sum method and:

$$Output\ factor = \frac{T_{BDFG}}{T_{IM}} \left[ \frac{1 + \frac{p_2}{p_1}}{1 + \frac{1}{n_r} + \frac{p_2}{p_1} \left( 1 + n_r \right)} \right] \quad (22)$$

for the sum method. The  $n_{r_{opt}}$  is defined using the method given in [1], with the assumption of unity power factor and small load angle operation. The turns ratio for maximum output power is given by:

$$n_{r_{opt}} = \left( \frac{p_1}{p_2} \right)^{\frac{1}{2}} \quad (23)$$

However, this is constant to the results obtained in [1]:

$$n_{r_{opt}} = \left( \frac{p_1}{p_2} \right)^{\frac{2}{3}} \quad (24)$$

The actual value of  $n_{r_{opt}}$  are 0.71 and 0.63 for the 4/8 brushless DFIG from equation (23) and (24).

#### ACKNOWLEDGMENT

The research leading to these results has received funding from the European Union's Seventh Framework Program managed by Research Executive Agency (FP7/2007-2013) under Grant Agreement N.315485.

#### REFERENCES

- [1] R. McMahon, X. Wang, E. Abdi, P. Tavner, P. Roberts and M. Jagiela, "The brushless DFIG as a generator in wind turbines," *Power Electronics and Motion Control Conference*, Slovenia, pp. 1859–1865, 2006.
- [2] T. Strous, X. Wang, H. Polinder, and J. Ferreira, "Brushless doubly fed induction machines: magnetic field analysis," *IEEE Transactions on Magnetics*, vol. 52, no. 11, pp. 1–10, Nov. 2016.
- [3] B. Gorti, G. Alexander and R. Spee, "A novel, cost-effective stand-alone generator system," *IEEE 4th AFRICON*, vol. 2, pp. 626–631, Sep. 1996.
- [4] A. Wallace, R. Spee, and H. Lauw, "The potential of brushless doubly-fed machines for adjustable speed drives," *IEEE Record of the Pulp and Paper Industry Technical Conference*, pp. 45–50, June. 1990.
- [5] F. Xiong and X. Wang, "Design and performance analysis of a brushless doubly-fed machine for stand-alone ship shaft generator systems," *Int. Conf. on Electrical and Control Eng.*, pp. 2114–2117, Sep. 2011.
- [6] P. Han, M. Cheng, S. Ademi and M. Jovanovic, "Brushless doubly-fed machines: Opportunities and challenges," *IEEE Chinese Journal of Electrical Engineering*, vol. 4, no. 2, pp. 1–17, July. 2018.
- [7] Y. Liao, L. Xu and L. Zhen, "Design of a doubly fed reluctance motor for adjustable-speed drives," *IEEE Transactions on Industry Applications*, vol. 32, no. 5, pp. 1195–1203, Sep. 1996.
- [8] I. Scian, D. Dorrell and P. Holik, "Assessment of losses in a brushless doubly-fed reluctance machine," *IEEE Transactions on Magnetics*, vol. 42, no. 10, pp. 3425–3427, Sep. 2006.
- [9] T. Fukami, M. Momiyama and K. Shima, "Steady-state analysis of a dual-winding reluctance generator with a multiple-barrier rotor," *IEEE Transactions on Energy Conversion*, vol. 23, no. 2, pp. 492–498, 2008.
- [10] M. Hsieh, I. Lin and D. Dorrell, "An analytical method combining equivalent circuit and magnetic circuit for BDFRG," *IEEE Transactions on Magnetics*, vol. 50, no. 11, pp. 1–5, Dec. 2014.
- [11] R. Rebeiro and A. Knight, "Design and torque capability of a ducted rotor brushless doubly fed reluctance machine," *IET Electric Power Application*, vol. 12 no. 7, pp. 1058–1064, April. 2018.
- [12] T. Staudt, F. Wurtz, L. Gerbaud, N. Batistela and P. Kuo-Peng, "An optimization-oriented sizing model for brushless doubly fed reluctance machines: Development and experimental validation," *Electric Power System Research, Elsevier*, vol. 132, pp. 125–131, March. 2016.
- [13] S. Ademi and M. Jovanovic, "Vector control methods for brushless doubly fed reluctance machines," *IEEE Transactions on Industrial Electronics*, vol. 61, pp. 96–104, May. 2015.
- [14] T. Strous, H. Polinder and J. Ferreira, "Brushless doubly-fed induction machines for wind turbines: developments and research challenges," *IET Electric Power Applications*, vol. 11, pp. 991–1000, July. 2017.
- [15] M. Matheka, S. Ademi and R. McMahon, "Brushless doubly fed machine magnetic field distribution characteristics and their impact on the analysis and design," *IEEE Transactions on Energy Conversion*, vol. 34, no. 4, pp. 2180–2188, Dec. 2019.
- [16] R. McMahon, E. Abdi, et. al., "Design and testing of a 250 kW medium-speed brushless DFIG," in *Power Electronics, Machines and Drives, 6th IET International Conference on*, pp. 1–6, March. 2012.
- [17] F. Runcos, R. Carlson, N. Sadowski, P. Kuo-Peng, and H. Voltolini, "Performance and vibration analysis of a 75 kW brushless double-fed induction generator prototype," in *Industrial Applications Conference, 41st IAS Annual Meeting*, vol. 5, pp. 2395–2402, Oct. 2006.
- [18] A. Oraee, E. Abdi, S. Abdi and R. McMahon, "A study of converter rating for the brushless DFIG," in *Renewable Power Generation Conference*, pp. 1–4, Sep. 2013.

- [19] H. Liu and L. Xu, "Design and performance analysis of a doubly excited brushless machine for wind power generator application," *IEEE Int. Symp. Power Electronics for Distributed Generation Systems*, pp. 597–601, June. 2010.
- [20] E. Abdi, R. McMahon, et. al., "Performance analysis and testing of a 250 kW medium-speed brushless doubly-fed induction generator," *IET Renewable Power Generation*, vol. 7, pp. 631–638, Nov. 2013.
- [21] R. McMahon, M. Mmamlatelo, W. Xiaoyan and M. Tatlow, "Design considerations for the brushless doubly-fed induction machine," *IET Electric Power Application*, vol. 10, no. 5, pp. 394–402, May. 2016.
- [22] A. Oraee, E. Abdi and R. McMahon, "Converter rating optimization for a brushless doubly fed induction generator," *IET Renewable Power Generation*, vol. 9, no. 4, pp. 360–367, Dec. 2015.
- [23] P. Roberts, T. Long, R. McMahon, S. Shao, E. Abdi, et. al., "Dynamic modelling of the brushless doubly fed machine," *IET Electric Power Applications*, vol. 7, no. 7, pp. 544–556, 2013.
- [24] S. Abdi, E. Abdi and R. McMahon, "Optimization of the magnetic circuit for brushless doubly fed machines," *IEEE Transactions on Energy Conversion*, vol. 30, no. 4, pp. 1611–1620, Sep. 2015.
- [25] R. McMahon, P. Roberts, et. al., "Rotor parameter determination for the brushless doubly fed induction machine," *IET Electric Power Applications*, vol. 9, no. 8, pp. 549–555, Sep. 2015.
- [26] A. Broadway and L. Burbridge, "Self-cascaded machine: a low-speed motor or high frequency brushless alternator," *Proceedings, Institution of Electrical Engineers*, vol. 117, no. 7, pp. 1227–1290, 1970.
- [27] S. Tohidi, P. Tavner, R. McMahon, et. al., "Low voltage ride-through of DFIG and brushless DFIG: similarities and differences," *Electric Power Systems Research*, vol. 110, pp. 64–72, May. 2014.



**Sul Ademi** (M'12) received the B.Eng. and Ph.D. degrees in electrical and electronics engineering from Northumbria University, Newcastle upon Tyne, U.K., in 2011 and 2014, respectively.

From 2015 to 2017, he was a Lead Researcher, engaged in knowledge exchange and transfer partnership activities between University of Strathclyde, Glasgow, U.K. and GE Grid Solutions, Stafford, U.K. He is currently a Research Scientist with the Warwick Manufacturing Group, University of Warwick, Coventry, U.K. His research interests include electric motor drives, control of doubly-fed machines, and design and analysis of novel permanent-magnet machines.



**Ashknaz Oraee** received the B.Eng. degree in electrical engineering from Kings College London, London, U.K., in 2011.

In 2015, she received her Ph.D. degree in electrical engineering from Cambridge University, U.K. focusing on electrical machine design and optimization. Her current research interests include electrical machines and drives for renewable power generation.



**Richard McMahon** received the B.A. degree in electrical sciences and the Ph.D. degree from the University of Cambridge, Cambridge, U.K., in 1976 and 1980, respectively.

Following post-doctoral work on semiconductor device processing, he became a University Lecturer in electrical engineering with the Engineering Department, University of Cambridge, in 1989, where he was a Senior Lecturer in 2000. In 2016, he joined the Warwick Manufacturing Group (WMG), University of Warwick, Coventry, U.K., as a Professor

of power electronics. His current research interests include electrical drives, power electronics, and semiconductor materials.



**Ehsan Abdi** (SM12) received the B.Sc. degree from the Sharif University of Technology, Tehran, Iran, in 2002, and the M.Phil. and Ph.D. degrees, from Cambridge University, Cambridge, U.K., in 2003 and 2006, respectively, all in electrical engineering.

He is currently the Managing Director of Wind Technologies Ltd., Cambridge, where he has been involved with commercial exploitation of the brushless doubly fed induction generator technology for wind power applications. His main research interests include electrical machines and drives, renewable

power generation, and electrical measurements and instrumentation



**Salman Abdi** received the B.Sc. degree from Ferdowsi University, Mashhad, Iran, in 2009, and the M.Sc. degree from the Sharif University of Technology, Tehran, Iran, in 2011, both in electrical engineering. He then completed the Ph.D. degree in electrical machines design and modelling from Cambridge University, Cambridge, U.K., in 2015.

He is currently a Lecturer in Electrical Engineering at the University of East Anglia, Norwich, U.K. His main research interests include electrical machines and drives for renewable power generation and automotive applications.

tomotive applications.